Generalization of the Numerov method for solution of *Nd* breakup problem in configuration space

V. M. Suslov* and B. Vlahovic†
Physics Department, North Carolina Central University, 1801 Fayetteville Street, Durham, North Carolina 27707, USA
(Received 10 December 2003; published 22 April 2004)

A new computational method for solving the configuration-space Faddeev equations for three-nucleon systems has been developed. This method is based on the spline decomposition in the angular variable and a generalization of the Numerov method for the hyperradius. The *s*-wave calculations of the inelasticity and phase shift as well as breakup amplitudes for *n-d* and *p-d* breakup scatterings for lab energies 14.1 and 42.0 MeV were performed with the Malfliet-Tjon I-III potential. In the case of *n-d* breakup scattering the results are in good agreement with those of the benchmark solution [J. L. Friar, B. F. Gibson, G. Berthold, W. Glöckle, Th. Cornelius, H. Witala, J. Haidenbauer, Y. Koike, G. L. Payne, J. A. Tjon, and W. M. Kloet, Phys. Rev. C **42**, 1838 (1990); J. L. Friar, G. L. Payne, W. Glöckle, D. Hüber, and H. Witala, Phys. Rev. C **51**, 2356 (1995)]. In the case of *p-d* quartet breakup scattering disagreement for the inelasticities reaches up to 6% as compared with those of the Pisa group [A. Kievsky, M. Viviani, and S. Rosati, Phys. Rev. C **64**, 024002 (2001)]. The calculated *p-d* amplitudes fulfill the optical theorem with a good precision.

DOI: 10.1103/PhysRevC.69.044003 PACS number(s): 21.45.+v, 11.80.Jy, 25.45.De

I. FADDEEV EQUATIONS IN CONFIGURATION SPACE

This paper deals with the *s*-wave breakup scattering in three-nucleon systems. Our approach is based on the method of the Faddeev equations [4], which was modified by Merkuriev to incorporate the Coulomb force [5]. The Faddeev components Ψ_α for three-body Coulomb systems satisfy the following set of differential Faddeev equations:

$$\{-\Delta_{\overline{x}_\alpha}-\Delta_{\overline{y}_\alpha}+V_c+V_\alpha(|\overline{x}_\alpha|)-E\}\Psi_\alpha(\overline{x}_\alpha,\overline{y}_\alpha) = -V_\alpha(|\overline{x}_\alpha|)\sum_{\beta\neq\alpha}\Psi_\beta(\overline{x}_\beta,\overline{y}_\beta), \quad (1)$$

where V_c and V_α are the Coulomb and nuclear potentials, respectively. The Coulomb potential has the following form:

$$V_c=\sum_\alpha \frac{n}{|x_\alpha|}\prod_{i\subset\alpha}\frac{1}{2}(1+\tau_z^i), \quad n=\frac{me^2}{\hbar^2}, \quad (2)$$

where $e^2=1.44$ MeV fm and $\hbar^2/m=41.47$ MeV fm^2. The sum runs over $\alpha=1,2,3$ for the three possible pairs and the product of the isospin projection operators runs over the indices i of the particles belonging to the pair α. As independent coordinates, we take the Jacobi vectors $\overline{x}_\alpha,\overline{y}_\alpha$. For the pair $\alpha=1$, they are related to particle coordinates by the formulas

$$\overline{x}_1=\overline{r}_2-\overline{r}_3, \quad \overline{y}_1=\frac{\overline{r}_2+\overline{r}_3}{2}-\overline{r}_1; \quad (3)$$

for $\alpha=2,3$ one has to make cyclic permutations of the indices in Eq. (3). The Jacobi vectors with different α's are linearly related by the orthogonal transformation

$$\begin{pmatrix}\overline{x}_\alpha\\ \overline{y}_\alpha\end{pmatrix}=\begin{pmatrix}C_{\alpha\beta} & S_{\alpha\beta}\\ -S_{\alpha\beta} & C_{\alpha\beta}\end{pmatrix}\begin{pmatrix}\overline{x}_\beta\\ \overline{y}_\beta\end{pmatrix}, \quad C_{\alpha\beta}^2+S_{\alpha\beta}^2=1, \quad (4)$$

where

$$C_{\alpha\beta}=-\sqrt{\frac{m_\alpha m_\beta}{(M-m_\alpha)(M-m_\beta)}},$$

$$S_{\alpha\beta}=(-)^{\beta-\alpha}\mathrm{sgn}(\beta-\alpha)\sqrt{1-C_{\alpha\beta}^2}, \quad M=\sum_{\alpha=1}^{3}m_\alpha. \quad (5)$$

To derive the equations to be used in numerical computations, we perform the partial-wave decomposition of Eq. (1) and separate the spin-isospin and angular variables (see, for instance, Refs. [6,7]). As a result, in the *s*-wave doublet case, the set (1) is reduced to a system of two integrodifferential equations. In the polar coordinates, $\rho^2=x^2+\frac{4}{3}y^2$ and $\tan\theta=(2/\sqrt{3})(y/x)$, it has the following form (here we omit the index 1):

$$\left\{-\frac{\partial^2}{\partial\rho^2}-\frac{1}{\rho^2}\frac{\partial^2}{\partial\theta^2}+V_c^t(\rho,\theta)+V^t(\rho,\theta)-\frac{1}{4\rho^2}-E\right\}U^t(\rho,\theta) = -\frac{1}{4}V^t(\rho,\theta)\int_{-1}^{+1}du\frac{\sin\theta\cos\theta}{\sin\theta'\cos\theta'} \times[U^t(\rho,\theta')-3U^s(\rho,\theta')],$$

$$\left\{-\frac{\partial^2}{\partial\rho^2}-\frac{1}{\rho^2}\frac{\partial^2}{\partial\theta^2}+V_c^s(\rho,\theta)+V^s(\rho,\theta)-\frac{1}{4\rho^2}-E\right\}U^s(\rho,\theta) = -\frac{1}{4}V^s(\rho,\theta)\int_{-1}^{+1}du\frac{\sin\theta\cos\theta}{\sin\theta'\cos\theta'} \times[-3U^t(\rho,\theta')+U^s(\rho,\theta')], \quad (6)$$

where

*Also at Department of Mathematical and Computational Physics, Sankt-Petersburg State University, 198504 Petrodvorets, Sankt-Petersburg, Russia. Electronic address: suslov@mph.phys.spbu.ru
†Electronic address: branko@jlab.org

$$\cos^2\theta'(u,\theta) = \frac{1}{4}\cos^2\theta - \frac{\sqrt{3}}{2}\cos\ \theta \sin\ \theta u + \frac{3}{4}\sin^2\theta, \quad (7)$$

and the first derivative in the radius is eliminated by the substitution $\Psi^{(t,s)} = \rho^{-1/2}U^{(t,s)}$. In Eq. (6), the *s*-wave Coulomb potential $V_c^{(t,s)}(\rho,\theta)$ is given by [7]

$$V_c^t(\rho,\theta) = \frac{n\mu^t(\theta)}{\rho}, \quad \mu^t(\theta) = \begin{cases} \dfrac{2}{\sqrt{3}\sin\ \theta}, & \theta > 30^\circ \\ \dfrac{2}{\cos\ \theta}, & \theta \leqslant 30^\circ \end{cases},$$

$$V_c^s(\rho,\theta) = \frac{n\mu^s(\theta)}{\rho}, \quad \mu^s(\theta) = \frac{1}{3}\left(\frac{2}{\cos\ \theta} + \mu^t(\theta)\right). \quad (8)$$

The Malfliet-Tjon I-III potential (see Refs. [1,2]) was chosen as the nuclear potential $V^{t,s}(\rho,\theta)$. The set of partial differential equations (6) must be solved for the functions satisfying the regularity conditions

$$U^{t,s}(0,\theta) = U^{t,s}(\rho,0) = U^{t,s}(\rho,\pi/2) = 0 \quad (9)$$

and the following asymptotic conditions [5]:

$$U^t|_{\rho\to\infty} \sim \sqrt{\rho}\varphi_d[\rho,\cos(\theta)]\left\{F_o\left(\gamma, p\frac{\sqrt{3}}{2}\rho\ \sin(\theta)\right) + a(p) \times\left[G_o\left(\gamma, p\frac{\sqrt{3}}{2}\rho\ \sin(\theta)\right) + iF_o\left(\gamma, p\frac{\sqrt{3}}{2}\rho\ \sin(\theta)\right)\right]\right\} + A^t(\theta)\exp\left[i\sqrt{E}\rho - i\frac{n\mu^t(\theta)}{2\sqrt{E}}\ln(2\sqrt{E}\rho)\right],$$

$$U^s|_{\rho\to\infty} \sim A^s(\theta)\exp\left[i\sqrt{E}\rho - i\frac{n\mu^s(\theta)}{2\sqrt{E}}\ln(2\sqrt{E}\rho)\right]. \quad (10)$$

Here, φ_d is the deuteron wave function, F_o and G_o are the regular and irregular Coulomb functions, $\gamma = 2n/3p$ is the Coulomb parameter with p the momentum in the center-of-mass system, and $\mu^{t,s}(\theta)$ is defined in Eqs. (8). The unknown functions $a(p)$ and $A^{t,s}$ are the elastic and breakup scattering amplitudes:

$$a(p) = \frac{\eta\ \exp(i2\delta) - 1}{2i}, \quad (11)$$

where η and δ are the inelasticity and phase shift, respectively. In the case of *n-d* breakup scattering, the asymptotic conditions retain the functional form of Eq. (10) but the Coulomb functions F_o and G_o should be replaced by sine and cosine, respectively.

II. NUMEROV METHOD AND SPLINE APPROXIMATION

Our previous calculations of elastic amplitudes for *n-d* and *p-d* breakup scatterings, in which the reduction of the Faddeev equations to an algebraic problem was performed by means of finite-difference approximation for the hyperradius, have demonstrated a weak dependence of the results on the choice of the matching radius [8]. Nevertheless, to get accurate results for breakup amplitudes, it is necessary to increase the cutoff radius considerably. To obtain accurate results at the same time, we applied the Numerov method for solving partial differential equations. The idea of Numerov method consists in using the initial differential equation to calculate higher derivatives in the expansion of the unknown function in Taylor's series. According to Numerov, one has to keep all terms up to the sixth derivative in this expansion. Summation of the equations for points $\rho-\Delta\rho$ and $\rho+\Delta\rho$ leads to the following finite-difference approximation of the second radial derivative:

$$\left.\frac{\partial^2 U(\rho,\theta)}{\partial\rho^2}\right|_{\rho_i} = \frac{U(\rho_{i+1},\theta) - 2U(\rho_i,\theta) + U(\rho_{i-1},\theta)}{\Delta\rho^2} - \frac{\Delta\rho^2}{12}U_\rho^{IV}(\rho_i,\theta) + O(\Delta\rho^4). \quad (12)$$

The fourth radial derivative of the Faddeev component has to be found by differentiating the second derivative in the corresponding Faddeev equation. From here on we make the analysis for the spin-quartet Faddeev equation. In the *s*-wave approach, this equation in the polar coordinates has the form [7]

$$\left\{-\frac{\partial^2}{\partial\rho^2} - \frac{1}{\rho^2}\frac{\partial^2}{\partial\theta^2} + V_c(\rho,\theta) + V^s(\rho,\theta) - \frac{1}{4\rho^2} - E\right\}U(\rho,\theta) = \frac{2}{\sqrt{3}}V(\rho,\theta)\int_{\theta^-}^{\theta^+} d\theta' U(\rho,\theta'), \quad (13)$$

where $\theta^- = |\theta - \pi/3|$ and $\theta^+ = \pi/2 - |\theta - \pi/6|$. Thus for the fourth derivative of the Faddeev component the following formula is to be obtained:

$$\frac{\partial^4 U(\rho,\theta)}{\partial\rho^4} = -\frac{\partial^2}{\partial\rho^2}\left[\left\{\frac{1}{\rho^2}\frac{\partial^2}{\partial\theta^2} - V_c(\rho,\theta) - V(\rho,\theta) + \frac{1}{4\rho^2} + E\right\} \times U(\rho,\theta) + \frac{2}{\sqrt{3}}V(\rho,\theta)\int_{\theta^-}^{\theta^+} d\theta' U(\rho,\theta')\right]. \quad (14)$$

The finite-difference approximation for the second derivative up to the fourth order in $\Delta\rho$ results from substitution of this expression into Eq. (12) as follows:

TABLE I. *n-d* and *p-d* elastic phase shifts and inelasticities.

	LA/Iowa Ref. [1]	Bochum Ref. [1]	Pisa Ref. [3]	Present work	Pisa Ref. [3]	Present work
14.1 Mev		Doublet	*n-d*		*p-d*	
Re(δ)	105.48	105.50	105.48	105.47	108.44	108.06
η	0.4648	0.4649	0.4649	0.4649	0.4984	0.4929
		Quartet	*n-d*		*p-d*	
Re(δ)	68.95	68.96	68.952	68.93	72.604	73.64
η	0.9782	0.9782	0.9782	0.9782	0.9795	0.9202
42 Mev		Doublet	*n-d*		*p-d*	
Re(δ)	41.34	41.37	41.341	41.34	43.667	43.47
η	0.5024	0.5022	0.5022	0.5022	0.5056	0.5071
		Quartet	*n-d*		*p-d*	
Re(δ)	37.71	37.71	37.722	37.70	39.947	39.19
η	0.9035	0.9033	0.9033	0.9034	0.9046	0.866

$$\left.\frac{\partial^2 U(\rho,\theta_j)}{\partial\rho^2}\right|_{\rho_i} = \frac{U(\rho_{i+1},\theta_j)-2U(\rho_i,\theta_j)+U(\rho_{i-1},\theta_j)}{\Delta\rho^2} + \frac{\Delta\rho^2}{12}\frac{\partial^2}{\partial\rho^2}\left[\left\{\frac{1}{\rho^2}\frac{\partial^2}{\partial\theta^2}-V_c(\rho,\theta)-V(\rho,\theta) + \frac{1}{4\rho^2}+E\right\}U(\rho,\theta) + \frac{2}{\sqrt{3}}V(\rho,\theta)\int_{\theta^-}^{\theta^+}d\theta' U(\rho,\theta')\right]_{\rho_i} + O(\Delta\rho^4). \tag{15}$$

Finally, replacement of the second radial derivative in the Faddeev equation by the obtained expression leads to the following generalized formula of Numerov method:

$$-\left[\frac{U(\rho_{i+1},\theta)-2U(\rho_i,\theta)+U(\rho_{i-1},\theta)}{\Delta\rho^2}-\left(1+\frac{\Delta\rho^2}{12}\frac{\partial^2}{\partial\rho^2}\right)\times\left\{-\frac{1}{\rho^2}\frac{\partial^2}{\partial\theta^2}+V_c(\rho,\theta)+V(\rho,\theta)-\frac{1}{4\rho^2}-E\right\}U(\rho,\theta)\right]_{\rho_i,\theta_j} = \frac{2}{\sqrt{3}}\left(1+\frac{\Delta\rho^2}{12}\frac{\partial^2}{\partial\rho^2}\right)\left[V(\rho,\theta)\int_{\theta^-}^{\theta^+}d\theta' U(\rho,\theta')\right]_{\rho_i,\theta_j}. \tag{16}$$

Modification of the Numerov method for the set of the differential equations, Eq. (6), does not present any difficulty in principle. However, due to unhandiness of the corresponding equations, we do not show them here. To ensure the accuracy of order $(\Delta\theta)^4$ for the approximation in the angular variable, Hermitian splines of the fifth degree have been used (see Ref. [9]). These splines are local and each spline $S_{\sigma i}(x)$ is defined for x belonging to two adjacent subintervals $[x_{i-1},x_i]$ and $[x_i,x_{i+1}]$. Their analytical form is fixed by the following smoothness conditions:

$$S_{\sigma i}(x_{i-1})=0, \quad S_{\sigma i}(x_{i+1})=0, \quad \sigma=0,1,2, \tag{17}$$

and

$$S_{0i}(x_i)=1, \quad S'_{0i}(x_i)=0, \quad S''_{0i}(x_i)=0,$$
$$S_{1i}(x_i)=0, \quad S'_{1i}(x_i)=1, \quad S''_{1i}(x_i)=0,$$
$$S_{2i}(x_i)=0, \quad S'_{2i}(x_i)=0, \quad S''_{2i}(x_i)=1. \tag{18}$$

To reduce the resulting equation (16) to an algebraic problem, one should explicitly calculate the derivatives with respect to ρ in Eq. (16) using the following spline expansion for the Faddeev component:

$$U(\rho,\theta)=\sum_{\sigma=0}^{2}\sum_{j=0}^{N_\theta+1}C_j^\sigma(\rho)S_{\sigma j}(\theta), \tag{19}$$

where $N_\theta+1$ is the number of internal subintervals for the angular variable $\theta\in[0,\pi/2]$. Upon substituting the spline expansion (19) into the Faddeev equation, we use a collocation procedure with three Gaussian quadrature points per subinterval. As the number of internal breakpoints for angular variable θ is equal to N_θ, the basis of quintic splines consists of $3N_\theta+6$ functions. Three of them should be excluded using the last two regularity conditions from (9) and continuity of the first derivative in θ of the Faddeev component at either $\theta=0$ or $\theta=\pi/2$, as the collocation procedure yields $3N_\theta+3$ equations.

III. METHOD OF PARTIAL INVERSION

Using the spline approximation in the angular variable and the Numerov method for the hyperradius leads to an algebraic problem for the unknown coefficients $C_j^\sigma(\rho_k)$. It is convenient to transform this problem back to the set of linear equations for the Faddeev components $U(\rho_i,\theta_k)$ by means of Eq. (19). Thus Eq. (16) is reduced to a matrix form

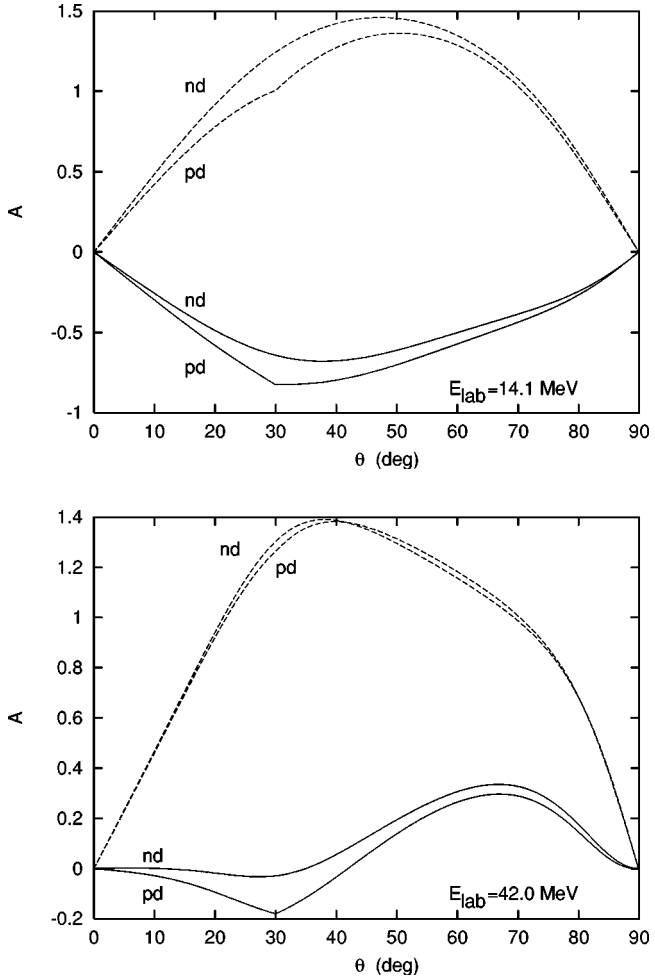

FIG. 1. Spin-quartet *n-d* and *p-d* breakup amplitudes. The dashed (solid) lines correspond to imaginary (real) part of the amplitudes.

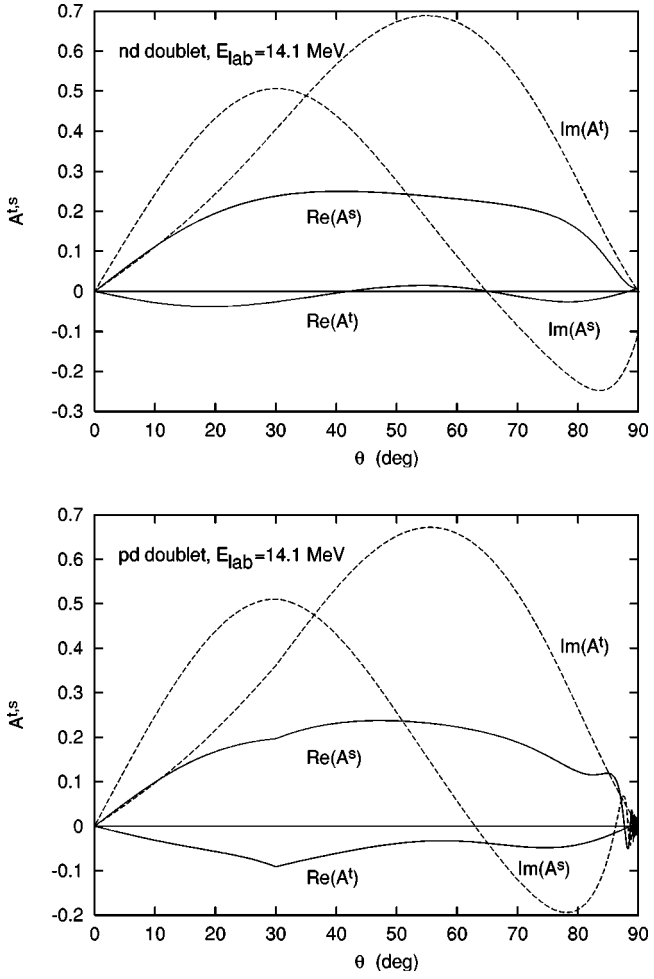

FIG. 2. Spin-doublet *n-d* and *p-d* breakup amplitudes for E_{lab} = 14.1 MeV. A^s is the singlet (pair spin $s=0$) breakup amplitude and A^t is the triplet (pair spin $s=1$) one.

$$(D * U)_i = -\delta_{in} D^+ U_{n+1}, \quad n = N_\rho. \tag{20}$$

The matrices D and D^+ are of dimension $N_\rho N_c \times N_\rho N_c$ and $N_c \times N_c$, respectively. Here, N_ρ is the number of breakpoints in the hyperradius ρ and $N_c = 3N_\theta + 3$ is the number of collocation points in the angular variable θ.

Matrix D has the tri-block-diagonal structure that optimizes considerably the inversion problem. Index $n+1$ stands for hyperradius $\rho_{n+1} = R_{max}$, where R_{max} is the cutoff radius at which the asymptotic conditions, Eqs. (10), are implemented. By formal inversion of the matrix D in Eq. (20), the solution of the problem may be written in the following form:

$$U_j = -D^{-1}_{jn} D^+ U_{n+1}, \quad j = 1,2, \ldots, N_\rho. \tag{21}$$

The form of this equation results from keeping the incoming wave in the asymptotic conditions (10). As a consequence, the right-hand part of Eq. (21) has a single nonzero term marked with index $n+1$. In Eq. (21) one should consider the last two components of vector U:

$$U_{n-1} = -D^{-1}_{n-1n} D^+ U_{n+1},$$

$$U_n = -D^{-1}_{nn} D^+ U_{n+1}. \tag{22}$$

Provided R_{max} is large enough, the vectors U_{n-1} and U_n on the left side of Eqs. (22) may be replaced by the corresponding vectors obtained by evaluating Eqs. (10) at the radii $\rho = \rho_{n-1}$ and $\rho = \rho_n$. As a result we obtain a set of linear equations for the unknown amplitudes a and $\mathcal{A}$:

$$a v_{n-1} + m_{n-1} \mathcal{A} = \mathcal{F}_{n-1},$$

$$a v_n + m_n \mathcal{A} = \mathcal{F}_n. \tag{23}$$

For the sake of brevity, we do not display here the explicit form of vectors $v_j, \mathcal{F}_j$ and matrices m_j. As $R_{max} \to \infty$ the set of equations (23) has a constant a as a solution. At finite R_{max} its solution is a vector a with generally different components corresponding to different angles. We follow the method of Merkuriev *et al.* [6], which consists in selecting the components of a in the region of the maximum of the deuteron wave function, where a turns out to be independent of the angle.

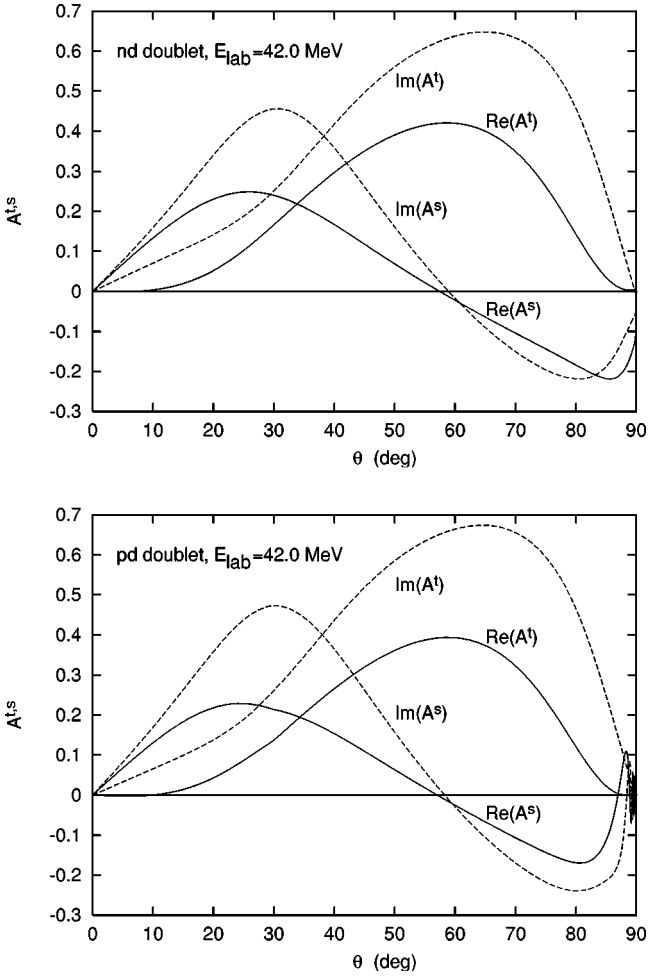

FIG. 3. Spin-doublet *n-d* and *p-d* breakup amplitudes for E_{lab} =42.0 MeV. Notations are the same as in Fig. 2.

Furthermore, we propose a new method for a more adequate calculation of the amplitudes. The set of linear equations (23) is overdetermined, since the number of equations is $2N_c$ and the number of unknowns is N_c+1. Therefore it is natural to use the least-squares method (LSM). One can apply it by two ways. In the first one, it is needed to express the breakup amplitude $\mathcal{A}$ from the lower equation (23) and substitute it into the upper one. As a result one has the following expression:

$$a \cdot \mathbf{v} = \mathbf{F}, \tag{24}$$

where vectors are defined as follows: $\mathbf{v}=v_{n-1}-m_{n-1}m_n^{-1}v_n$ and $\mathbf{F}=\mathcal{F}_{n-1}-m_{n-1}m_n^{-1}\mathcal{F}_n$. According to LSM one should minimize the following functional:

$$\|a \cdot \mathbf{v} - \mathbf{F}\|^2 = \min. \tag{25}$$

Differentiating this expression in Re a and Im a we obtain

$$a = \frac{(\mathbf{v}^*, \mathbf{F})}{(\mathbf{v}^*, \mathbf{v})}, \tag{26}$$

where (ξ^*, f) is an ordinary scalar product.

In the second way, it is needed to express the elastic amplitude a from the lower equation (23) using the scalar product:

$$a = \frac{(v_n^*, \mathcal{F}_n - m_n\mathcal{A})}{(v_n^*, v_n)}. \tag{27}$$

Substituting a from Eq. (27) into the upper Eq. (23) leads to the following set of linear equations:

$$m_{n-1}\mathcal{A} - v_{n-1}\frac{(v_n^*, m_n\mathcal{A})}{(v_n^*, v_n)} = \mathcal{F}_{n-1} - v_{n-1}\frac{(v_n^*, \mathcal{F}_n)}{(v_n^*, v_n)}. \tag{28}$$

The explicit form of Eq. (28) is as follows:

$$\sum_{j=1}^{N_c}\left\{m_{n-1,ij} - \frac{v_{n-1,i}}{(v_n^*, v_n)}\sum_{k=1}^{N_c} v_{n,k}^* m_{n,kj}\right\}\mathcal{A}_j = \mathcal{F}_{n-1,i} - v_{n-1,i}\frac{(v_n^*, \mathcal{F}_n)}{(v_n^*, v_n)}, \quad i = 1, \ldots, N_c. \tag{29}$$

Solving the set in Eq. (29), we get the breakup amplitude $\mathcal{A}$. Substituting the obtained breakup amplitude into Eq. (27), one may compute the elastic amplitude a. Note that one can apply Eq. (27) to calculate the elastic amplitude a either in the components or via a scalar product. In the first case, the components of a are practically equal to a constant for all angles $\theta \in (0, \pi/2)$ and this constant coincides with the value of a calculated by using the scalar product to the fourth decimal. It should also be noted that the elastic amplitudes calculated by the method from Ref. [6] and LSM coincide

TABLE II. *n-d* and *p-d* spin-quartet reduced breakup amplitudes E_{lab}=14.1 Mev. The numbers in square brackets denote powers of 10.

θ(deg)	0	10	20	30	40	50	60	70	80
Present work, *n-d* results, $R_{max}\to\infty$									
Re($^3S_1$)	−1.91[−1]	−1.93[−1]	−1.94[−1]	−1.89[−1]	−1.75[−1]	−1.58[−1]	−1.47[−1]	−1.51[−1]	−1.78[−1]
Im($^3S_1$)	3.65[−1]	3.67[−1]	3.70[−1]	3.72[−1]	3.73[−1]	3.81[−1]	4.00[−1]	4.32[−1]	4.62[−1]
LA/Iowa, *n-d* results, $R_{max}\to\infty$, Ref. [2]									
Re($^3S_1$)	−1.92[−1]	−1.93[−1]	−1.94[−1]	−1.89[−1]	−1.75[−1]	−1.58[−1]	−1.47[−1]	−1.51[−1]	−1.78[−1]
Im($^3S_1$)	3.65[−1]	3.67[−1]	3.70[−1]	3.72[−1]	3.73[−1]	3.81[−1]	4.00[−1]	4.31[−1]	4.62[−1]
Present work, $p-d$ results, $R_{max}\to\infty$									
Re($^3S_1$)	−2.21[−1]	−2.24[−1]	−2.31[−1]	−2.44[−1]	−2.07[−1]	−1.82[−1]	−1.68[−1]	−1.71[−1]	−1.96[−1]
Im($^3S_1$)	3.21[−1]	3.19[−1]	3.14[−1]	2.99[−1]	3.34[−1]	3.57[−1]	3.83[−1]	4.14[−1]	4.39[−1]

TABLE III. *n-d* and *p-d* spin-quartet reduced breakup amplitudes $E_{lab}=42.0$ MeV. The numbers in square brackets denote powers of 10.

θ(deg)	0	10	20	30	40	50	60	70	80
				Present work, *n-d* results, $R_{max}\to\infty$					
Re($^3S_1$)	1.48[−2]	1.65[−3]	−3.11[−2]	−3.12[−2]	7.76[−2]	2.52[−1]	4.51[−1]	6.53[−1]	6.98[−1]
Im($^3S_1$)	1.69[−0]	1.74[−0]	1.87[−0]	1.92[−0]	1.80[−0]	1.67[−0]	1.70[−0]	1.94[−0]	2.52[−0]
				LA/Iowa, *n-d* results, $R_{max}\to\infty$, Ref. [2]					
Re($^3S_1$)	1.48[−2]	9.22[−4]	−3.21[−2]	−3.09[−2]	7.70[−2]	2.52[−1]	4.51[−1]	6.53[−1]	6.93[−1]
Im($^3S_1$)	1.69[−0]	1.74[−0]	1.87[−0]	1.92[−0]	1.80[−0]	1.68[−0]	1.70[−0]	1.95[−0]	2.52[−0]
				Present work, *p-d* results, $R_{max}\to\infty$					
Re($^3S_1$)	−8.22[−2]	−1.09[−1]	−1.83[−1]	−2.56[−1]	−3.83[−2]	1.81[−1]	3.90[−1]	5.78[−1]	5.85[−1]
Im($^3S_1$)	1.67[−0]	1.72[−0]	1.83[−0]	1.86[−0]	1.79[−0]	1.70[−0]	1.74[−0]	1.99[−0]	2.54[−0]

with this constant to the same accuracy. To control the accuracy of calculations, all methods are used.

IV. RESULTS OF THE CALCULATIONS

The elastic amplitude a and breakup amplitude $\mathcal{A}$ for *n-d* and *p-d* scatterings were computed at $E_{lab}=14.1$ and 42.0 MeV. The following values were used for the parameters of the calculation: $N_\rho\sim 10\,000$, $N_\theta\sim 600$, and values of the hyperradius R_{max} as large as 800 fm. In Table I, the elastic phase-shifts δ and inelasticities η are presented for various energies and spin cases. As one can see from Table I, our results for *n-d* breakup are in very good agreement with calculations of other groups. However, for *p-d* breakup, they differ from those of the Pisa group [3]. To see the influence of the Coulomb interaction on *p-d* breakup scattering as compared to *n-d* one, we calculated the *n-d* and *p-d* breakup amplitudes $\mathcal{A}(\theta)$ for the total spin $S=3/2$ (spin-quartet case) and $\mathcal{A}^{t,s}(\theta)$ for the total spin $S=1/2$ (spin-doublet case). Our results are shown in Figs. 1–3.

It is important to note that in our *s*-wave approach higher partial waves of the Coulomb potential have not been taken into account. Nevertheless, the accuracy of this approach is about 1% for energies exceeding 1 MeV as was already pointed out by Merkuriev *et al.* in Ref. [10]. From Fig. 1, it follows that the Coulomb interaction has a noticeable effect on the real and imaginary parts of the *p-d* quartet breakup amplitude at $E_{lab}=14.1$ MeV, especially for angles in the vicinity of $\pi/3$. At $E_{lab}=42.0$ MeV, the effect of the Coulomb interaction is perceptible only in the real part of the amplitude. In the spin-doublet case, a substantial effect of the Coulomb interaction persists for the energy $E_{lab}=14.1$ MeV. As one can see in Fig. 2, a large enough influence of the Coulomb force is noticeable for the real part of both the singlet and triplet breakup amplitudes. At $E_{lab}=42.0$ MeV, a small influence of the Coulomb interaction is felt in the behavior of the singlet breakup amplitude for angles exceeding $\pi/3$ (see Fig. 3). Oscillations of the singlet breakup amplitudes for angles in a small vicinity of $\pi/2$ reflect the behavior of the breakup part in the singlet asymptotic condition in

TABLE IV. *n-d* and *p-d* spin-doublet reduced breakup amplitudes $E_{lab}=14.1$ MeV. The numbers in square brackets denote powers of 10.

θ(deg)	0	10	20	30	40	50	60	70	80
				Present work, *n-d* results, $R_{max}\to\infty$					
Re(^1S)	8.81[−2]	8.61[−2]	8.04[−2]	7.29[−2]	6.65[−2]	6.42[−2]	6.84[−2]	8.42[−2]	1.11[−1]
Im(^1S)	1.84[−1]	1.81[−1]	1.72[−1]	1.50[−1]	1.14[−1]	7.18[−2]	2.59[−2]	−3.49[−2]	−1.76[−1]
Re($^3S_1$)	−2.44[−2]	−2.21[−2]	−1.59[−2]	−7.77[−3]	−3.46[−4]	4.75[−3]	5.21[−3]	−2.31[−3]	−1.82[−2]
Im($^3S_1$)	8.00[−2]	8.44[−2]	9.79[−2]	1.20[−1]	1.48[−1]	1.76[−1]	2.00[−1]	2.14[−1]	2.09[−1]
				LA/Iowa, *n-d* results, $R_{max}\to\infty$, Ref. [2]					
Re(^1S)	8.79[−2]	8.59[−2]	8.03[−2]	7.28[−2]	6.65[−2]	6.41[−2]	6.84[−2]	8.43[−2]	1.11[−1]
Im(^1S)	1.84[−1]	1.82[−1]	1.72[−1]	1.50[−1]	1.14[−1]	7.19[−2]	2.60[−2]	−3.49[−2]	−1.78[−1]
Re($^3S_1$)	−2.43[−2]	−2.21[−2]	−1.60[−2]	−7.89[−3]	−4.11[−4]	4.68[−3]	5.10[−3]	−2.40[−3]	−1.82[−2]
Im($^3S_1$)	8.01[−2]	8.45[−2]	9.80[−2]	1.20[−1]	1.48[−1]	1.76[−1]	1.99[−1]	2.14[−1]	2.09[−1]
				Present work, *p-d* results $R_{max}\to\infty$					
Re(^1S)	7.97[−2]	7.65[−2]	6.96[−2]	6.06[−2]	6.18[−2]	6.24[−2]	6.62[−2]	7.42[−2]	7.45[−2]
Im(^1S)	1.87[−1]	1.86[−1]	1.75[−1]	1.52[−1]	1.12[−1]	6.65[−2]	1.59[−2]	−5.10[−2]	−1.49[−1]
Re($^3S_1$)	−2.57[−2]	−2.48[−2]	−2.34[−2]	−2.73[−2]	−1.53[−2]	−8.79[−3]	−7.87[−3]	−1.55[−2]	−3.11[−2]
Im($^3S_1$)	6.95[−2]	7.37[−2]	8.66[−2]	1.07[−1]	1.40[−1]	1.70[−1]	1.95[−1]	2.10[−1]	2.02[−1]

TABLE V. *n-d* and *p-d* spin-doublet reduced breakup amplitudes $E_{lab}=42.0$ MeV. The numbers in square brackets denote powers of 10.

θ(deg)	0	10	20	30	40	50	60	70	80
				Present work, *n-d* results, $R_{max}\to\infty$					
Re(^{1}S)	5.01[−1]	4.94[−1]	4.59[−1]	3.63[−1]	2.19[−1]	8.78[−2]	−3.49[−2]	−2.10[−1]	−7.04[−1]
Im(^{1}S)	5.56[−1]	5.90[−1]	6.70[−1]	6.67[−1]	4.63[−1]	2.08[−1]	−2.58[−2]	−2.99[−1]	−8.13[−1]
Re(^{3}S$_1$)	−1.30[−2]	1.41[−2]	1.01[−1]	2.41[−1]	3.85[−1]	5.08[−1]	6.20[−1]	7.00[−1]	5.69[−1]
Im(^{3}S$_1$)	2.64[−1]	2.66[−1]	2.85[−1]	3.69[−1]	5.39[−1]	7.23[−1]	9.34[−1]	1.25[−0]	1.70[−0]
				LA/Iowa, *n-d* results, $R_{max}\to\infty$, Ref. [2]					
Re(^{1}S)	5.01[−1]	4.94[−1]	4.59[−1]	3.62[−1]	2.19[−1]	8.78[−2]	−3.50[−2]	−2.10[−1]	−7.05[−1]
Im(^{1}S)	5.56[−1]	5.91[−1]	6.70[−1]	6.66[−1]	4.63[−1]	2.09[−1]	−2.57[−2]	−2.99[−1]	−8.14[−1]
Re(^{3}S$_1$)	−1.30[−2]	1.33[−2]	1.00[−1]	2.42[−1]	3.85[−1]	5.07[−1]	6.20[−1]	7.00[−1]	5.69[−1]
Im(^{3}S$_1$)	2.63[−1]	2.66[−1]	2.85[−1]	3.70[−1]	5.39[−1]	7.23[−1]	9.34[−1]	1.25[−0]	1.70[−0]
				Present work, *p-d* results, $R_{max}\to\infty$					
Re(^{1}S)	4.95[−1]	4.84[−1]	4.35[−1]	3.24[−1]	2.02[−1]	8.06[−2]	−4.02[−2]	−2.17[−1]	−6.76[−1]
Im(^{1}S)	5.94[−1]	6.27[−1]	7.05[−1]	6.93[−1]	4.71[−1]	2.03[−1]	−4.41[−2]	−3.39[−1]	−8.90[−1]
Re(^{3}S$_1$)	−2.61[−2]	6.74[−4]	8.23[−2]	1.97[−1]	3.44[−1]	4.70[−1]	5.82[−1]	6.48[−1]	4.87[−1]
Im(^{3}S$_1$)	2.43[−1]	2.47[−1]	2.77[−1]	3.84[−1]	5.63[−1]	7.55[−1]	9.73[−1]	1.29[−0]	1.74[−0]

Eqs. (10) since the essential singularity occurs for the angle $\theta=\pi/2$.

In Tables II and III, our results for reduced quartet breakup amplitudes are presented. These amplitudes are defined in Ref. [2], as follows:

$$\mathcal{A}_{red}(\theta)=\frac{\mathcal{A}(\theta)K^2}{\sin(\theta)\cos(\theta)},\quad K^2=mE/\hbar^2. \tag{30}$$

As one can see from Tables II and III in the spin-quartet case, the agreement between our results and those of the Los-Alamos and Bochum groups, Ref. [2], is excellent (in Tables II–V, we do not show the results of the Bochum group since they practically coincide with those of the Los-Alamos one). It should be noted that one cannot explicitly calculate the reduced breakup amplitude for the angle $\theta=\pi/2$ because it is necessary to resolve an uncertainty in Eq. (30) for this angle. It is impossible numerically, since the breakup amplitude for the angle $\theta=\pi/2$ cannot be calculated using the Faddeev equations with sufficient accuracy in principle and one has to use another way to calculate it (for example, to exploit an integral representation from Ref. [6]). Unfortunately, there is no possibility to compare our results for the *p-d* quartet amplitudes because of absence of others in literature. In Tables IV and V, the reduced doublet breakup amplitudes are presented. The agreement between our results and those of Los-Alamos and Bochum groups [2] is again excellent. From these tables one can again see a large enough influence of the Coulomb interaction for the *p-d* doublet reduced amplitudes. In view of the large enough Coulomb effects in the case of spin-quartet breakup scattering, it is undoubtedly of interest to see it in more detail. In Fig. 4, the spin-quartet reduced breakup amplitudes are presented. Obviously, the Coulomb interaction effects are noticeable in the behavior of these amplitudes in the entire angular range, especially for lab energy $E_{lab}=14.1$ MeV.

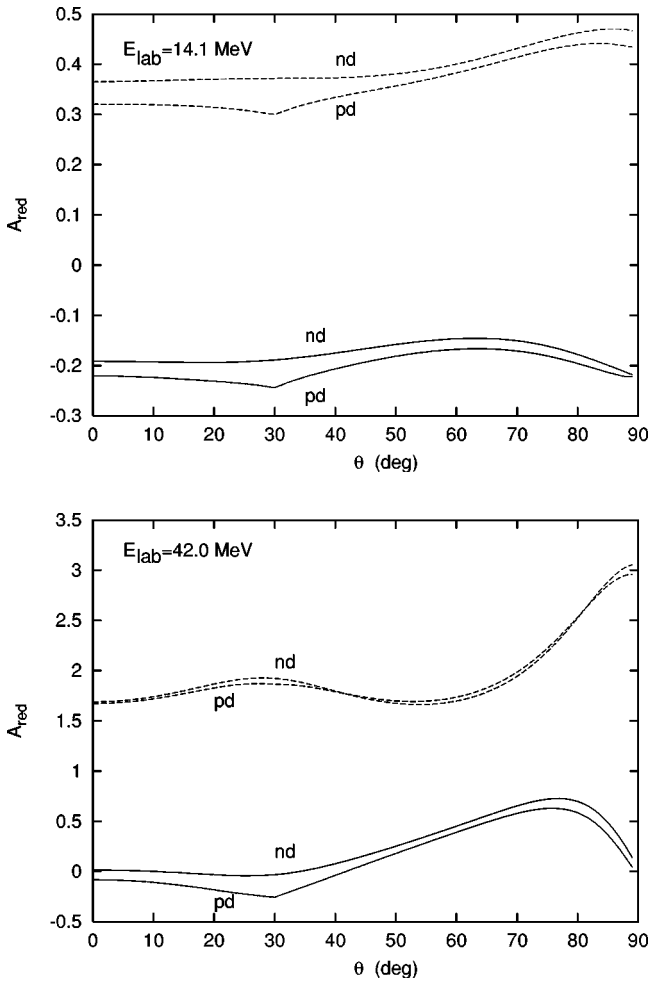

FIG. 4. Reduced quartet breakup amplitudes. The dashed (solid) lines correspond to imaginary (real) part of the amplitudes.

TABLE VI. The optical theorem results.

E_{lab}	*nd* quartet		*pd* quartet		*nd* doublet		*pd* doublet	
(MeV)	lhs	rhs	lhs	rhs	lhs	rhs	lhs	rhs
14.1	0.8626	0.8626	0.8871	0.8776	0.6994	0.6994	0.6991	0.7061
42.0	0.3860	0.3860	0.4127	0.4086	0.4679	0.4679	0.4864	0.4881

This effect should be important for the calculation of the total breakup amplitude, which should be quite different for *n-d* and *p-d* breakup scatterings.

To verify our results, optical theorem [6] is applied. In the spin-quartet case for the *s*-wave approach, it reads

$$\mathrm{Im}^4 a_0(p) = |a_0(p)|^2 + \frac{K}{p}\int_0^{\pi/2} d\theta A^*_{tot}\mathcal{A},$$

$$A_{tot}(\theta) = \mathcal{A}(\theta) - \frac{2}{\sqrt{3}}\int_{\theta^-}^{\theta^+} d\theta' \mathcal{A}(\theta'). \tag{31}$$

For the spin-doublet case in the *s*-wave approach (Ref. [6]), the optical theorem reads

$$\mathrm{Im}^2 a_0(p) = |a_0(p)|^2 + \frac{K}{p}\left\{\int_0^{\pi/2} d\theta [A^{*t}_{tot}\mathcal{A}^t + A^{*s}_{tot}\mathcal{A}^s]\right\},$$

$$A^t_{tot}(\theta) = \mathcal{A}^t(\theta) + \frac{1}{\sqrt{3}}\left\{\int_{\theta^-}^{\theta^+} d\theta' [\mathcal{A}^t(\theta') - 3\mathcal{A}^s(\theta')]\right\},$$

$$A^s_{tot}(\theta) = \mathcal{A}^s(\theta) + \frac{1}{\sqrt{3}}\left\{\int_{\theta^-}^{\theta^+} d\theta' [\mathcal{A}^s(\theta') - 3\mathcal{A}^t(\theta')]\right\}. \tag{32}$$

In Table VI, our optical theorem results are presented. Table

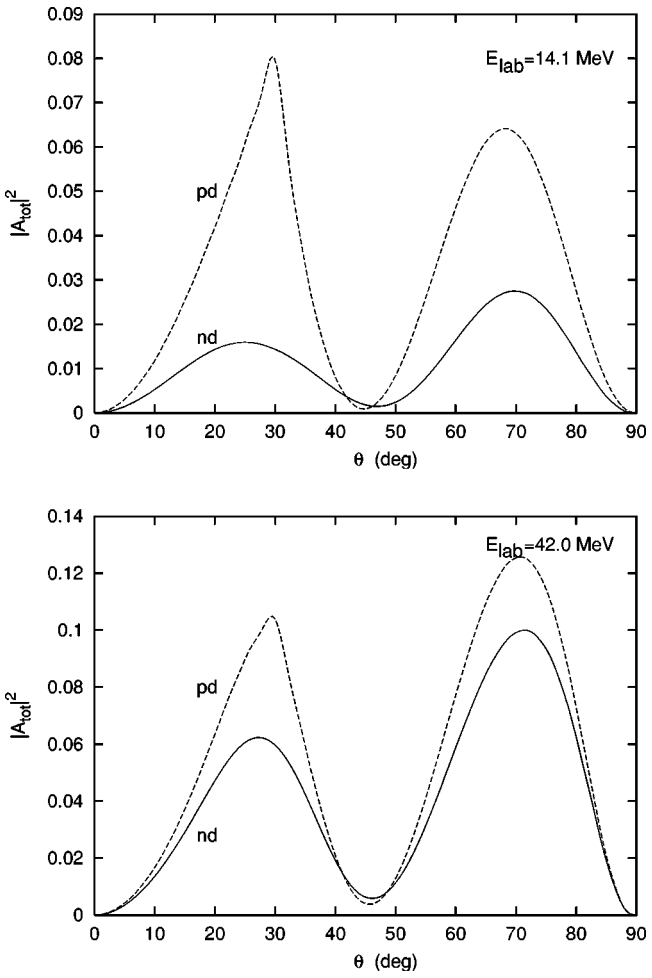

FIG. 5. Squares of the module of the physical quartet breakup amplitudes.

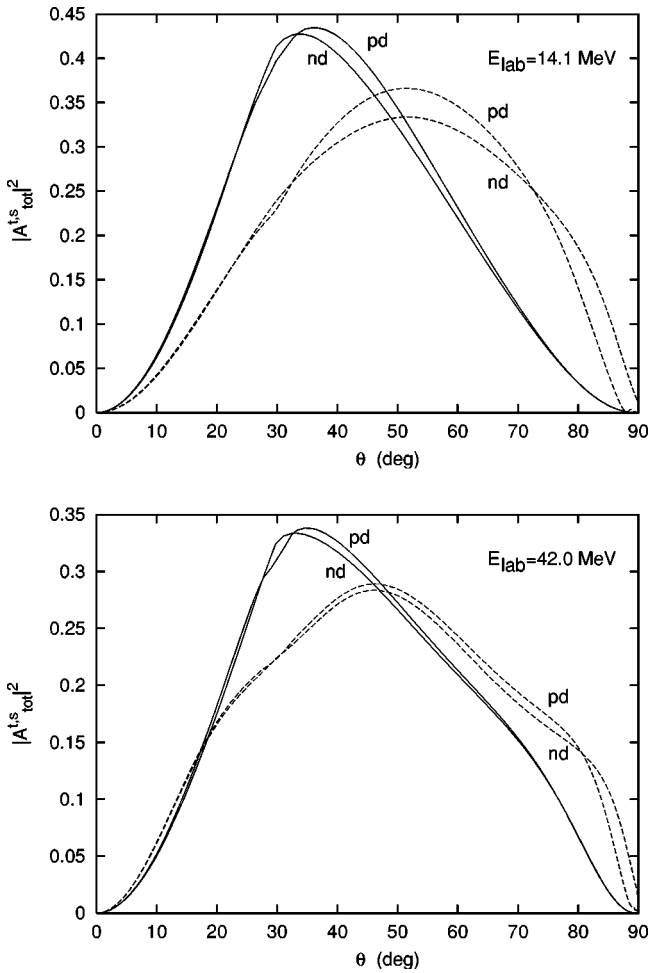

FIG. 6. Squares of the module of the physical doublet breakup amplitudes. The solid lines correspond to the spin-triplet amplitudes (pair spin $s=1$). The dashed lines correspond to the spin-singlet amplitudes (pair spin $s=0$).

TABLE VII. The quartet optical theorem results.

E_{lab} (MeV)	*nd*	*pd*
14.1	0.9999	0.9621
42.0	0.9999	0.9835

VI clearly confirms the accuracy of our results and the estimation of Merkuriev *et al.* [10] of the contribution of higher Coulomb partial waves under an *s*-wave approach, which is less than 1%. In Figs. 5 and 6, the physical *n-d* and *p-d* breakup amplitudes are depicted. The physical *p-d* quartet breakup amplitudes clearly demonstrate the influence of the Coulomb interaction, though they themselves have a small magnitude. For the doublet scattering, the Coulomb interaction has a smaller effect on the breakup amplitudes. The magnitude of these amplitudes is large as compared with the quartet ones. Therefore, the differential cross sections of the *n-d* and *p-d* processes should have some difference.

To directly study the dependence of the optical theorem results on the inelasticity in the spin-quartet case, we rewrite the first equation in Eqs. (31) in another form using the definition of the elastic amplitude, Eq. (11),

$$1 = \eta^2 + 4\frac{K}{p}\int_0^{\pi/2} d\theta A_{tot}^{*} A. \tag{33}$$

The results presented in Table VII show that our *n-d* amplitudes fulfill the optical theorem with a very high accuracy. In the case of *p-d* breakup scattering, the accuracy is a little bit worse. It is a consequence of our truncation of the partial-wave decomposition of the Coulomb potential. Analyzing Eq. (33) and the *n-d* and *p-d* quartet results for inelasticities of the Pisa group from Table I, one inevitably comes to the conclusion about the equality of the contributions from integral terms of the optical theorem for the *n-d* and *p-d* breakup processes. On the other hand, our quartet breakup amplitudes are quite different for these two reactions as one can see in Fig. 7, which is hardly compatible with the equality of these contributions. This casts some doubts on the Pisa results for the *p-d* quartet breakup scattering.

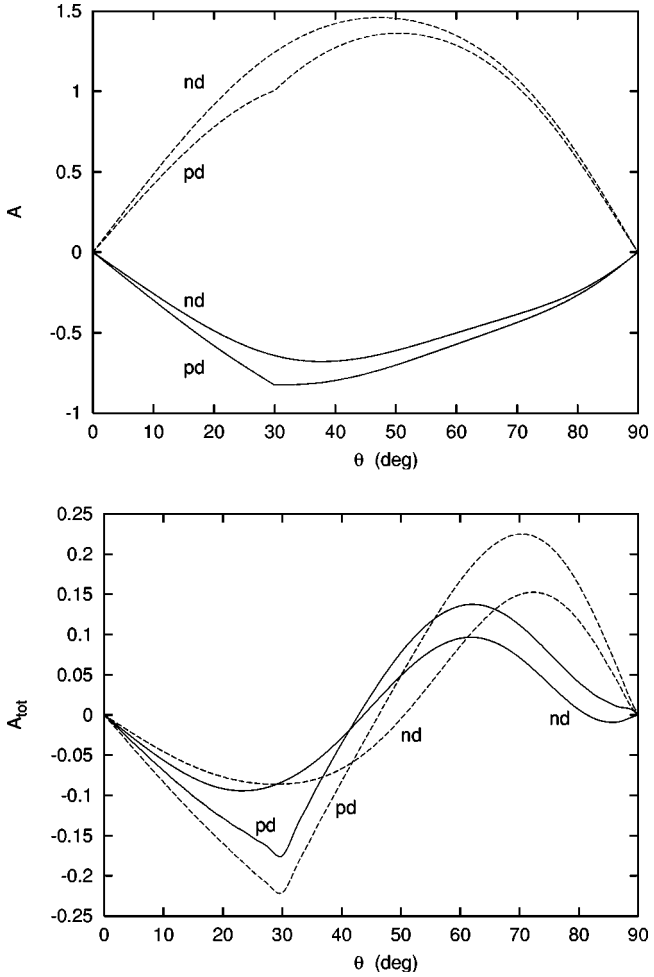

FIG. 7. The quartet breakup and total amplitudes for E_{lab} = 14.1 MeV. The dashed (solid) lines correspond to imaginary (real) part of the amplitudes.

V. CONCLUSION

We have shown that by using the Numerov method very accurate calculations can be performed with minimal computation resources (PC).

By retaining the incident wave in the asymptotics for the Faddeev components, unnecessary additional computations are eliminated casting the problem in a form that enables partial inversion.

The stability of our solutions for relatively large values of R_{max} illustrates its advantages for the investigation of the asymptotic behavior of solutions. In fact, the Numerov method allows us to compute the breakup amplitudes as well as the Faddeev components with a high accuracy for R_{max} = 800 fm and more.

The disagreement of our results for the phase shifts and inelasticities with those of the Pisa group in the *p-d* spin-quartet case reaches up to 6% as one can see from Table I. It cannot be explained by truncation of the partial-wave expansion of the Coulomb interaction in our calculation since the error introduced by neglecting higher partial Coulomb waves should not exceed 1% as it follows from the optical theorem results in Table VI.

ACKNOWLEDGMENTS

The authors wish to thank M. A. Braun for useful discussion and J. L. Friar for clear explanation on the breakup amplitude extrapolation. The work of B.V. and V.M.S. was supported in part by the U.S. Department of Defense under Grant No. 19-01-1-0795. and that of V.M.S. was partially supported by the RFFI under Grant No. 02-02-16562.

[1] J. L. Friar, B. F. Gibson, G. Berthold, W. Glöckle, Th. Cornelius, H. Witala, J. Haidenbauer, Y. Koike, G. L. Payne, J. A. Tjon, and W. M. Kloet, Phys. Rev. C **42**, 1838 (1990).
[2] J. L. Friar, G. L. Payne, W. Glöckle, D. Hüber, and H. Witala, Phys. Rev. C **51**, 2356 (1995).
[3] A. Kievsky, M. Viviani, and S. Rosati, Phys. Rev. C **64**, 024002 (2001).
[4] S. P. Merkuriev and L. D. Faddeev, *Quantum Scattering Theory for Few-Particle Systems* (Nauka, Moscow, 1985) (in Russian).
[5] S. P. Merkuriev, Ann. Phys. (N.Y.) **130**, 3975 (1980); Acta Phys. Austriaca, Suppl. **XXIII**, 65 (1981).
[6] S. P. Merkuriev, C. Gignoux, and A. Laverne, Ann. Phys. (N.Y.) **99**, 30 (1976).
[7] Yu. A. Kuperin, S. P. Merkuriev, and A. A. Kvitsinsky, Sov. J. Nucl. Phys. **37**, 1440 (1983).
[8] V. M. Suslov, A. Soldi, and B. Vlahovic, Few-Body Syst. **32**, 219 (2003).
[9] A. A. Kvitsinsky and C.-Y. Hu, Few-Body Syst. **12**, 7 (1992).
[10] A. A. Kvitsinsky, Yu. A. Kuperin, S. P. Merkuriev, A. K. Motovilov, and S. L. Yakovlev, Fiz. Elem. Chastits At. Yadra **17**, 267 (1986).